ACS ES&T Engineering

pubs.acs.org/estengg

Article

Competing Ion Behavior in Direct Electrochemical Selenite Reduction

Shiqiang Zou and Meagan S. Mauter*

Cite This: *ACS EST Engg.* 2021, 1, 1028–1035

Read Online

ABSTRACT: Anthropogenic selenium (Se) released in industrial and agricultural wastewaters presents toxicity challenges for local ecosystems. Se direct electrochemical reduction (SeDER) is an effective and thermodynamically favorable approach for Se(IV) removal, but evaluating the feasibility of SeDER in application requires a comprehensive understanding of system performance in complex water matrices. This study evaluates both the cathodic and anodic competing ion behavior in a SeDER process, including both four- and six-electron Se(IV) reduction pathways. The results suggest that sulfate promotes electrochemical Se(IV) removal efficiency by 11−23%, but nitrate hinders Se(IV) removal (2−11% decrease) by occupying cathodic reaction sites. The anodic competing ions, especially chloride, decrease SeDER performance by generating strong oxidants and disrupting Se(IV) reduction pathways. We also find that four-electron Se(IV) reduction outperforms its six-electron counterpart when treating simulated flue-gas desulfurization wastewater (with 7 g L^{-1} Cl^-), with a lowest effluent Se level of 0.23 mg L^{-1}, a highest removal efficiency of 96.9%, and a threshold deposition capacity of 3.5 g m^{-2} in a 7-day semicontinuous operation. Electrochemical Se(IV) removal using our prototype batch reactor is not competitive for treating low-Se concentration agricultural wastewaters (up to 24% removal). The results suggest the need for future work to evaluate alternative electrodes and reactor design that reduce water splitting reactions, enhance Faradaic efficiency, and promote mass transfer to the electrode surface.

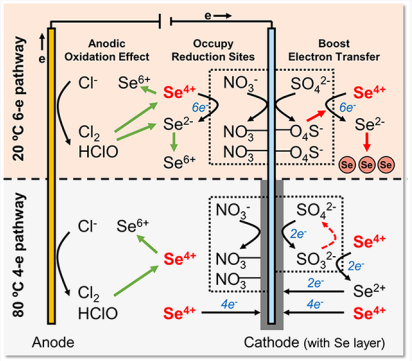

KEYWORDS: *Direct electrochemical reduction, Selenium removal, Electrodeposition, Competing ion behavior, Chronoamperometry*

INTRODUCTION

Aquatic selenium (Se) pollution is closely associated with anthropogenic activities,[1] including agricultural irrigation, mining and thermoelectric power generation, and high-tech fabrication and manufacturing industries.[2] Se is typically discharged into the aquatic environment as Se(IV) and Se(VI) oxyanions (e.g., SeO_3^{2-} and SeO_4^{2-}),[3] though other less predominant species such as selenocyanates ($SeCN^-$) and metal selenide (MeSe) are found in agriculture and power plant wastewaters.[4,5] Our limited understanding of Se toxicity and ecological risk meant that Se emissions were unmonitored and unregulated for decades.[6,7] More recently, research has documented the ecological effects of Se bioavailability in local ecosystems, including bioaccumulation in the food chain and Se toxicosis. For instance, the Se level in plants and animals at Kesterson Reservoir (San Joaquin Valley, California) was 100 times higher than those at the reference sites and accompanied by high incidences of wildlife mortality and embryonic deformity.[8]

To effectively control anthropogenic Se release, more than 30 full-scale biological and physicochemical Se treatment processes (e.g., ABMet and Selen-IX)[9,10] have been implemented in North America between 2007 and 2018.[11] Biological systems are characterized by a large footprint, constant chemical dosing, and susceptibility to performance upsets stemming from both environmental and operational changes. Biological processes can also generate toxic hydrogen selenide and organic Se species with significantly higher bioavailability than inorganic SeO_3^{2-} and SeO_4^{2-}. Physicochemical processes are capable of consistently meeting discharge limits, but low Se selectivity necessitates high rates of chemical dosing and increases capital and operational costs. Further, all existing Se removal technologies generate large amounts of (bio)solids that require further management and may cause secondary pollution from spent material transport and landfill leachate.[12,13] The need for cost reduction, energy savings, resource conservation, and regulation compliance motivate the development of advanced control technologies to address the emerging Se contamination.

We have recently reported an alternative strategy for Se direct electrochemical reduction (SeDER) that requires no

Received: March 16, 2021
Revised: April 9, 2021
Accepted: April 13, 2021
Published: April 22, 2021

https://doi.org/10.1021/acsestengg.1c00099
ACS EST Engg. 2021, 1, 1028–1035

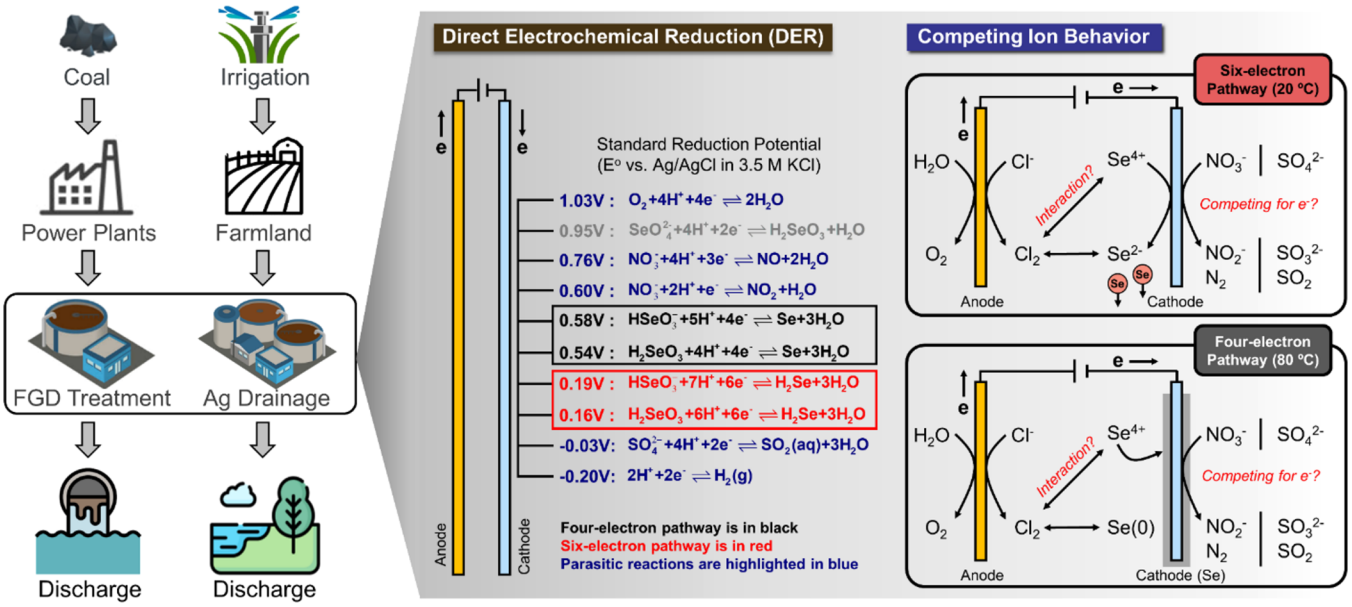

Figure 1. Direct electrochemical reduction can effectively remove Se(IV) from aqueous solution but requires comprehensive understanding of competing ion behavior in complex wastewaters.

chemical additives and significantly reduces solids generation.[14] SeDER is thermodynamically favored due to a very positive standard reduction potential for both Se(VI) and Se(IV) oxyanions, but Se(VI) reduction is significantly hindered by molecular-level structure reorganization and high activation energy. On the other hand, Se(IV) is readily electrochemically reduced and separated from the aqueous solution through a four- or six-electron pathway, with the former plating Se(0) directly onto the electrode surface and the latter producing Se(-II) that is chemically converted to Se(0). We previously reported that the four-electron Se(IV)/Se(0) pathway is a surface-limited process below 70 °C that terminates when the cathode is fully covered with the insulative amorphous Se(0). By raising the solution temperature above the amorphous to crystalline transition temperature at approximately 80 °C, continuous deposition of conductive crystalline Se(0) on the electrode can be achieved via the four-electron pathway. At 80 °C, the six-electron Se(IV)/Se(-II) reduction also operates continuously with linear kinetics, but the formed Se(0) suspended particles require further separation via gravitational settling or filtration. These past results indicated that the robust SeDER process can effectively treat 0.001−10 mM Se(IV) in diluted single-component solution (pH 4−7), with up to 95% removal efficiency in a prototype batch reactor.

While SeDER processes offer potential for continuous Se removal in a single-component aquatic environment, industrial and agricultural wastewaters are complex solution matrices containing many other anions. For instance, the concentrations of chloride, nitrate, and sulfate in flue-gas desulfurization (FGD) wastewater from coal-fired power plants range from 20 to 20,000 mg L^{-1} and can be several orders of magnitude higher than that of Se oxyanions (~1 mg L^{-1}).[15,16] The presence of these competing ions often triggers parasitic reactions in electrochemical systems, including capacitive deionization,[17] electron-Fenton processs,[18] and electrochemical advanced oxidation.[19] Anodic parasitic reactions (other than oxygen evolution reaction) could generate strong oxidants (e.g., chlorine gas, Cl_2) and react with reactants, intermediates, and products.[20,21] On the cathode side, nitrate and sulfate may directly compete with Se oxyanions for electrons.[22] These competing ions, accompanied by their anodic, cathodic, and subsequent solution-phase parasitic reactions, will decrease the Faradaic efficiency, increase the energy consumption, generate undesirable byproducts, and induce corrosion at the electrode (Figure 1). Hence, evaluating the potential for SeDER to treat Se-laden wastewaters requires a comprehensive understanding of the mechanisms and effect of competing ions on process efficiency and removal.

The present work comprehensively evaluates competing ion behavior in both the four- and six-electron Se(IV)DER reduction pathways. The specific aims of this study are to (1) investigate cathodic competing ion behavior of nitrate and sulfate, (2) understand the anodic competing ion behavior of chloride, (3) evaluate the Se deposition capacity and removal consistency with a regenerated electrode (i.e., after the deplating process), and (4) quantify the extent of Se removal in simulated FGD wastewater and agricultural drainage. The results from this study will probe parasitic reactions in simulated industrial and agricultural water matrices and help engineers and policy makers to retrofit current treatment trains to meet more stringent Se discharge regulations.

MATERIALS AND METHODS

Setup of the Three-Electrode Electrochemical System. Detailed information on the electrochemical cells can be found in our previous paper.[14] Briefly, each cell has an effective volume of 100 mL and a 3-D printed lid to reduce evaporation. For each experiment, the cell is filled with 100-mM phosphate-buffered saline (PBS) spiked with defined concentrations of sodium selenite (Na_2SeO_3), sodium chloride (NaCl), sodium nitrate ($NaNO_3$), sodium sulfate (Na_2SO_4), and/or sodium bicarbonate ($NaHCO_3$). The initial solution pH is adjusted to 5.5 to simulate a representable pH of industrial and agricultural wastewaters. Gold (Au) foil (Fisher Scientific, 1 × 5 × 0.125 cm, purity >99.9975%), a leakless miniature Ag/AgCl electrode (eQAD, Model ET072), and a platinum wire (CH Instrument, Model CHI 115) are used as the working

https://doi.org/10.1021/acsestengg.1c00099
ACS EST Engg. 2021, 1, 1028−1035

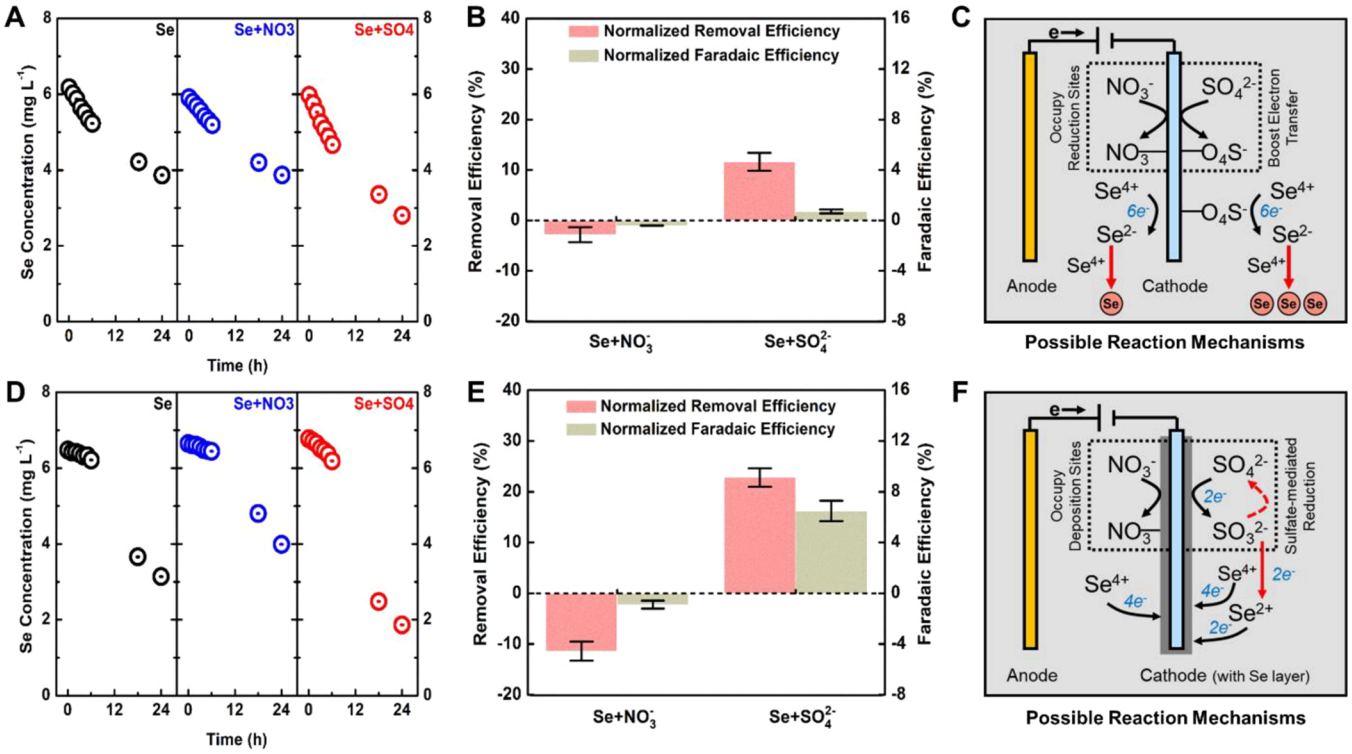

Figure 2. Cathodic competing ion behavior in a six-electron Se(IV) reduction pathway at 20 °C regarding (A) total soluble Se concentration profile, (B) normalized Se removal and Faradaic efficiencies, and (C) possible reaction mechanisms, or in a four-electron Se(IV) reduction pathway at 80 °C regarding (D) total soluble Se concentration profile, (E) normalized Se removal and Faradaic efficiencies, and (F) possible reaction mechanisms. The black and red arrows in C and F represent electrochemical and chemical reaction routes, respectively.

electrode, reference electrode, and the counter electrode, respectively. Note that selection and design of the electrodes are not the focus of this paper but are likely to be a fruitful area of future research. About 3.5 cm of the Au electrode is submerged in the solution, resulting in an effective reaction area of 7 cm^2. This three-electrode system is connected to an electrochemical potentiostat (BioLogic VSP-300) to conduct voltammetry and amperometry. A magnetic stirrer was placed inside the electrochemical cell (300 rpm) to enhance mass transfer. For experiments performed at elevated temperature, the electrochemical cell is heated in a sand bath. All chemicals were purchased from Fisher Scientific and used directly without further purification (purity >99.8%). Water was from a well-maintained Millipore Milli-Q system.

Experimental Procedure. We first investigated the cathodic competing ion behavior in the SeDER process. The blank control system contained 0.1 mM sodium selenite (~7 mg L^{-1} Se^{4+}) in a 100 mL PBS solution, whereas a two-component solution matrix contains a 0.1 mM sodium selenite PBS solution spiked with either 10 mM nitrate (~110 mg L^{-1} N) or 20 mM sulfate (~740 mg L^{-1} S). Note that all matrices used in this study were well buffered with 100-mM PBS to ensure a stable solution pH of 5.45−5.55 throughout the experiment. Chronoamperometry (CA) was initiated either at −0.6 V (vs Ag/AgCl reference) to sustain a six-electron Se(IV) reduction pathway under 20 °C or at −0.2 V (vs Ag/AgCl) for a four-electron Se(IV) reduction pathway under a solution temperature of 80 °C. Note that the same CA protocol was applied to all the tests in this study, with cathode potential being controlled for either a four- or a six-electron Se(IV) reduction pathway. Each batch test lasted for 24 h, with 1 mL water samples periodically taken from the electrochemical cell. Between each batch test, the Au electrode was electrochemically cleaned by holding at a potential of 1.1 V for 20 min to ensure thorough oxidation of surface deposits (i.e., deplating of Se(0) layer) in a separate 100-mM PBS solution. Detailed information on electrode regeneration can be found in Figure S1 and Video 1 (Supporting Information, SI sections 1 and 2). The regenerated Au electrode was then scanned from 0.3 to 1.5 V under a linear sweep voltammetry (LSV) to confirm complete removal of all residues.

We then investigated the anodic competing ion behavior of chloride in a two-component solution matrix. As above, the blank control system contained only 0.1 mM sodium selenite in PBS, while the experimental system was spiked with either 7 g L^{-1} or 16 g L^{-1} chloride. The operation and electrode regeneration protocols were the same as in the prior cathodic experiments. For both cathodic and anodic competing ion behavior experiments, water samples were filtered (if needed) to remove suspended Se(0) and preserved under 4 °C before quantification of soluble Se and other anion levels. Duplicate tests were performed in each experiment to ensure data accuracy and consistency.

Subsequently, we evaluated SeDER performance in simulated FGD wastewater through a four- or six-electron reduction pathway. Our simulated FGD wastewater used 100-mM PBS solution as the substrate to sustain a weakly acidic environment (pH = 5.5) and contained 7.0 mg L^{-1} Se(IV), 7.0 g L^{-1} Cl^-, 6.4 g L^{-1} SO_4^{2-}−S, 100.0 mg L^{-1} NO_3^-−N, 0.3 mg L^{-1} PO_4^{3-}−P, and 120 mg L^{-1} HCO_3^-. This composition was informed by the average ion concentrations from 10 coal-fired power plant FGD wastewater streams sampled between 2009 and 2013.[23] We ran a semicontinuous operation for 7 days under 80 °C to sustain a four-electron Se(IV) reduction. Note

https://doi.org/10.1021/acsestengg.1c00099
ACS EST Engg. 2021, 1, 1028−1035

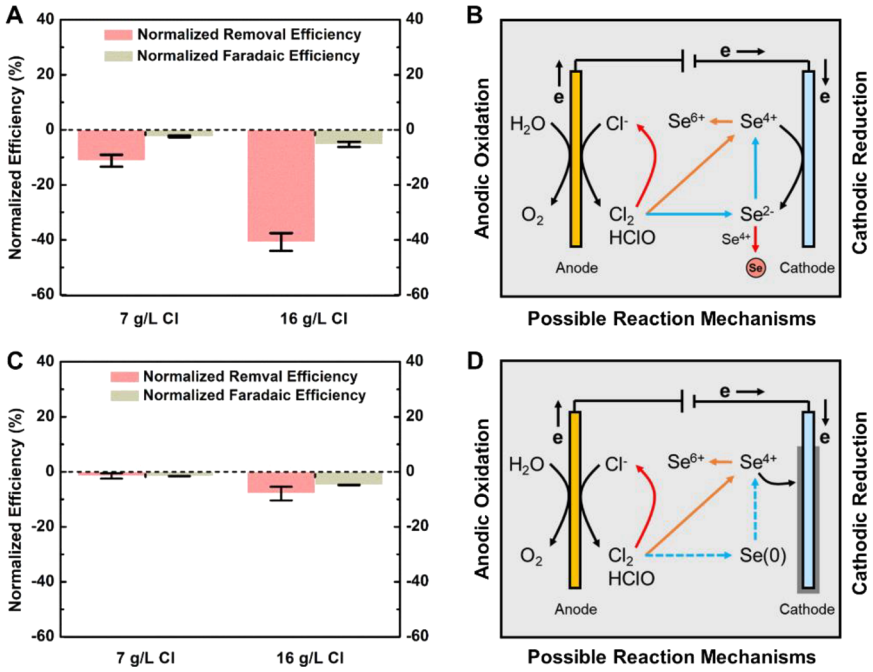

Figure 3. Anodic competing ion behavior in a six-electron Se reduction pathway at 20 °C regarding (A) normalized Se removal and Faradaic efficiencies and (B) possible reaction mechanisms, or in a four-electron Se reduction pathway at 80 °C regarding (C) normalized Se removal and Faradaic efficiencies and (D) possible reaction mechanisms. The black and colorful arrows in (B) and (D) stand for electrochemical and chemical reaction routes, and dashed lines represent possible reaction routes.

that we did not explore long-term four-electron Se(IV) reduction under 20 °C due to self-limiting deposition of insulative Se(0).[14] For each 24-h cycle, the treated simulated FGD wastewater was completely discharged, and 100 mL of fresh FGD wastewater was supplied to maintain a 7-ppm of Se(IV) level. The Au electrode was not regenerated throughout this semicontinuous operation, and samples were taken at the beginning and end of each 24-h cycle. Following a similar protocol, we then evaluated Se removal performance in the simulated FGD wastewater through a six-electron pathway at either 20 or 80 °C.

Finally, we explored SeDER performance on simulated agricultural drainage. Two different compositions of agricultural drainage were tested in this study, including raw drainage and drainage concentrated by reverse osmosis (RO) treatment with 50% water recovery. The simulated raw drainage contained 70 μg L^{-1} Se(IV), 3.6 g L^{-1} Cl, 5.1 g L^{-1} SO_4^{2-}−S, 200.0 mg L^{-1} NO_3^-−N, 0.3 mg L^{-1} PO_4^{3-}−P, and 120 mg L^{-1} HCO_3^-. The ion levels are doubled for the concentrated drainage. The compositions of simulated raw and concentrated drainage are based on the concentration of Grassland Drainage Area (1986−2009) from Panoche Drainage District, California.[24] Water samples were taken at the beginning and ending point of each 24-h operation.

Analytical Methods. Current, electrode potential, and energy consumption data from LSV and CA tests are recorded by the BioLogic potentiostat using the EC-Lab software (BioLogic Sciences Instruments). Total soluble Se concentration in the solution is quantified by inductively coupled plasma mass spectrometry (ICP-MS). Other ion concentrations, including nitrate, sulfate, nitrite, and chloride, are determined by Ion Chromatograph (Dionex ICS 6000). Quantification of performance metrics, including Se removal efficiency (%), Se removal rate (mg h^{-1} m^{-2}), Se deposition capacity (g m^{-2}), and Faradaic efficiency (%), can be found in the Supporting Information (SI section 3, eqs S1−S5).

RESULTS AND DISCUSSION

Cathodic Competing Ion Behavior. Nitrate and sulfate oxyanions are ubiquitous in industrial and agricultural wastewaters, exist at concentrations 10 to 10 000 times that of Se oxyanions, and have standard reduction potentials comparable to those of Se (Figure 1). Quantifying the implications of competing ion behavior in SeDER systems is critical to assessing the functional performance of this process. We first investigated cathodic competing ion behavior of nitrate and sulfate in a six-electron Se(IV) reduction pathway (−0.6 V vs Ag/AgCl). The blank control group exhibited a 41.6% Se(IV) removal efficiency at 20 °C, resulting in an effluent Se level of 3.86 mg L^{-1} (Figure 2A). The presence of 110 mg L NO_3^-−N decreased the Se removal efficiency by 2.8% (Figure 2B) and the Faradaic efficiency by 0.4%. A stable nitrate concentration over the 24-h operation indicates negligible nitrate reduction to nitrite on a Au electrode (0 mg L^{-1}, Figure S2A, SI Section 4), which is a kinetically constrained process without a catalyst.[25] Hence, we believe that nitrate decreases the Se(IV) reduction rate not by consuming electrons on a cathode but through physical adsorption to the electrode surface (Au−$NO_{3,ads}$, Figure 2C) and competition with Se(IV) for reduction sites (Au−$SeO_{3,ads}$).

In contrast with nitrate, the presence of 640 mg L^{-1} SO_4^{2-}−S significantly enhances Se(IV) conversion to Se(-II). We observe an 11.6% increase in removal efficiency (Figure 2B) and a small 0.7% increase in Faradaic efficiency. Sulfate concentration remains constant throughout the experiment, indicating no Faradaic sulfate reduction (Figure S2A). While a comprehensive assessment of surface mediated reactions is beyond the scope of this paper, these results suggest that the

https://doi.org/10.1021/acsestengg.1c00099
ACS EST Engg. 2021, 1, 1028−1035

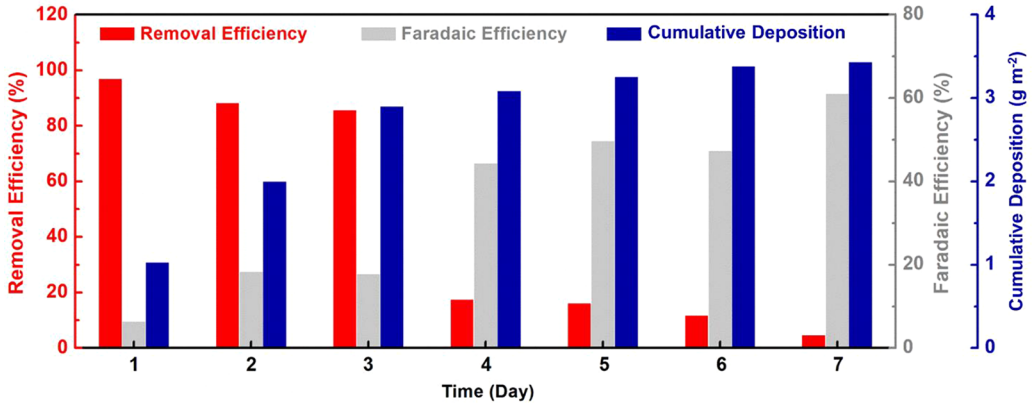

Figure 4. Electrochemical Se(IV) reduction and removal performance in simulated FGD wastewater. The system was operated under semicontinuous operation with no cathode regeneration. Removal and Faradaic efficiencies were quantified every 24 h, whereas the cumulative deposition was determined over the entire operating time.

surface-adsorbed sulfate (Au-$SO_{4,ads}^-$, Figure 2C) may transfer electrons to Se(IV) more efficiently than a bare Au surface.

In a four-electron Se(IV) reduction pathway at 80 °C (−0.2 V vs Ag/AgCl), we are able to plate elemental Se(0) from the solution phase, resulting in a 51.6% removal efficiency and an effluent Se(IV) concentration of 3.48 mg L^{-1} in the blank control group (Figure 2D). Note that this plating process converts the Au cathode to a conductive Se(0) interface and influences both the form of surface-adsorbed oxyanions (e.g., Se−$SeO_{3,ads}^-$, Se−$NO_{3,ads}$, or Se−$SO_{4,ads}^-$) and the rate of Se deposition. In the presence of 110 mg L^{-1} NO_3^-−N, we observed an 11.4% decrease in Se(IV) removal efficiency and a minor 0.9% decrease in the Faradaic efficiency relative to the blank control (Figure 2E). On the basis of the consistent nitrate concentration and 0 mg L^{-1} nitrite production (Figure S2B, SI section 4), we believe that the adsorbed nitrate (either Au−$NO_{3,ads}$ or Se−$NO_{3,ads}$) occupies Se reduction sites and hinders efficient Se plating (Figure 2F). This hindering effect is stronger than that observed in the six-electron pathway, potentially due to a higher affinity between NO_3^- and a Se surface relative to a Au surface. The slow and unstable adsorption of −NO_3 on Au is evidenced by a low Au−O bond energy (of Au−$NO_{3,ads}$) on the volcano plot.[26] In contrast, 680 mg L^{-1} SO_4^{2-}−S significantly enhances both Se removal and Faradaic efficiencies (22.8% and 6.5%, respectively), suggesting an increased portion of electrons is diverted to Se(IV) reduction. We hypothesize that conductive crystalline Se(0) may partially catalyze sulfate reduction to sulfite at 80 °C and that the generated sulfite further reacts with Se(IV) to produce selenotrithionate (Se^{2+}) and sulfate (eq 1).[27,28] This sulfate-mediated Se(IV) reduction has been reported in previous partitioning and speciation studies in FGD wastewater.[29,30]

$$HSeO_3^- + 3HSO_3^- = Se(SO_3)_2^{2-} + SO_4^{2-} + 2H_2O \quad (1)$$

The produced selenotrithionate (Se^{2+}) facilitates Se(0) plating through either a two-electron transfer process or a self-cleaving process (eq 2).[31]

$$Se(S_2O_3)_2^{2-} = Se(0) + S_4O_6^{2-} \quad (2)$$

The generated reduced form of sulfur (e.g., $S_4O_6^{2-}$) could be reoxidized on the anode, keeping the soluble sulfur at a stable level (Figure S2B).

To summarize, sulfate promotes electrochemical Se(IV) removal in both four- and six-electron pathways, but nitrate slightly hinders Se(IV) removal by occupying reaction sites. By evaluating cathodic competing ion behavior, we discover that the robust SeDER can selectively remove Se(IV) from a complex water matrix containing high levels of sulfate and nitrate. Our results also warrant future research to better understand the fundamental mechanisms, thermodynamics, and kinetics of sulfate-mediated Se(IV) reduction at the electrode surface.

Anodic Competing Ion Behavior. Most industrial and agricultural wastewaters contain high levels of chloride (Cl^-), which can be oxidized to chlorine gas (Cl_2) in electrochemical systems. The generated Cl_2 may further react with H_2O to produce hypochlorous acid (HClO). Both Cl_2 and HClO are strong oxidants and may interact with Se species. Hence, we need to understand the anodic behavior of Cl^- and its impact on the SeDER process in simple single-chamber reactor designs. In the blank control group, the six-electron pathway removes 45.2% Se(IV) at 20 °C and exhibits a Faradaic efficiency of 5.7%. In the presence of 7 g L^{-1} Cl^-, we observe a 11.2% decrease in Se removal efficiency and a 2.4% decrease in Faradaic efficiency relative to the blank control system with 0 g L^{-1} Cl (Figure 3A). A further increase of Cl^- concentration to 16 g L^{-1} results in a 40.8% decrease in Se removal efficiency and a 5.3% decrease in Faradaic efficiency. These results indicate that the presence of Cl^- and generated chlorine-based oxidants will greatly hinder SeDER in single-chamber electrochemical systems, potentially by initiating solution-phase oxidation of Se(IV) to Se(VI) and Se(-II) to Se(IV) (Figure 3B).[32,33] When treating wastewater containing high Cl^- levels, we would recommend a two-chamber electrochemical system to separate anodic and cathodic reactions and prevent chlorine-based oxidants in the catholyte.

In contrast, we observe less of an impact of Cl^- on four-electron Se(IV) reduction. The blank control exhibits 55.2% Se(IV) removal, with a 1.5% and 7.9% decrease in removal efficiency in the presence of 7 and 16 g L^{-1} Cl^-, respectively (Figure 3C). This minor performance drop may result from direct oxidation of Se(IV) to Se(VI) in the solution phase. Elemental Se(0) can be dissolved in nitric acid and perchloric acid,[34] but no previous study has confirmed Se(0) dissolution in hypochlorous acid (HClO) or aqueous chorine gas ($Cl_{2,aq}$). Given that the majority of Se(IV) will be directly plated as Se(0) on the electrode surface, the outer Se(0) layer further shields the inner Se(0) layer from the chlorine-based oxidants

https://doi.org/10.1021/acsestengg.1c00099
ACS EST Engg. 2021, 1, 1028−1035

(e.g., Cl_2 and HClO; Figure 3B). Compared to the six-electron pathway, the four-electron pathway has a higher tolerance to chlorine-laden wastewaters and may be a better alternative for Se removal in flue-gas desulfurization wastewaters (under a typical safe operating range for FGD systems of 6.2 to 16 mg L^{-1} Cl^-).[15,16]

Electrochemical Se(IV) Removal in Simulated FGD Wastewater. While we have separately investigated the cathodic and anodic competing ion behaviors in two-component solution systems, it is crucial to quantify the extent of Se(IV) removal in complex water matrices. Hence, we conduct a 7-day semicontinuous operation to treat simulated FGD wastewater through a four-electron pathway, with no electrode regeneration in between, to further quantify the threshold Se(0) deposition capacity. We use a regenerated (or "pre-conditioned", SI section 2) Au cathode and successfully removed about 96.9% Se(IV) on the first day (Figure 4). The Se(IV) level in the effluent drops from 7.45 mg L^{-1} to 0.23 mg L^{-1}, indicating a Se removal rate of 147.1 mg h^{-1} m^{-2} and a deposition capacity of 1.03 g m^{-2}. On the second and third day, we observe continuous deposition of Se(0) on the cathode, resulting in an effluent Se level of 0.90 mg L^{-1} and 1.06 mg L^{-1}, respectively. The daily removal efficiency is relatively consistent for these 2 days (88.3% and 85.6%), with a cumulative Se deposition of 2.00 and 2.90 g m^{-2}. Beyond 3 g m^{-2} cumulative Se deposition, Se(IV) removal slows dramatically, and on the fourth day the removal efficiency drops to 17.5%.

The maximum cumulative deposition is approximately 3.5 g m^{-2}. This trend suggests self-limiting deposition where a thick layer of conductive Se(0) induces a significant potential drop on the cathode surface (i.e., lower electric driving force) that disrupts the four-electron Se(IV) reduction pathway. We also observe an increasing trend in Faradaic efficiency (from 2.7% to 61.1% over the 7-day experiment), which is related to the significant potential drop toward the end of the 7-day operation and the resulting reduction in parasitic reactions at the cathode surface (mainly the hydrogen evolution reaction).

The 7-day operation results demonstrate that the four-electron pathway effectively removes Se(IV) from a complex water matrix, even in the presence of 6.4 g L^{-1} SO_4^{2-}, 110 mg L^{-1} NO_3^-–N, and 7 g L^{-1} Cl^-. By depositing conductive Se(0), we are able to demonstrate a continuously operated treatment process to selectively remove Se(IV). Electrode regeneration is required beyond a 3.0 g m^{-2} deposition capacity and can be achieved either through mechanical scaping or periodic electrochemical oxidation to restore Se removal performance. Note that no suspended Se(0) is generated over the 7-day operation, significantly minimizing the solid management and disposal costs. This solid-free operation also ensures excellent effluent quality (i.e., negligible turbidity) and a compact system footprint (i.e., no need for a downstream membrane separation).

We also evaluate SeDER performance in simulated FGD wastewater using a six-electron pathway, either under 20 °C to yield insulative amorphous red Se(0) or under 80 °C to generate conductive crystalline gray Se(0). As before, no electrode regeneration is performed between each test. Interference from 7 g L^{-1} Cl in simulated FGD wastewater resulted in a Se removal efficiency of only 33.7% at 20 °C on the first day (Figure S3A, SI section 5), with an effluent Se level of 4.62 mg L^{-1}. Further operation in the second and third day revealed a 2–3% daily drop in removal efficiency, owing to the gradual occupation of Se adsorption sites by surface-attached insulative Se(0) and reduced mass transport to the electrode surface (Figure S3B, SI section 5). We can remove a majority of the attached Se(0) via sonication, minimizing the daily efficiency drop to 0.5% on the fourth day.

While performing the six-electron pathway at an elevated operating temperature of 80 °C would reduce the issues associated with insulative Se(0) deposition, doing so also accelerates the anodic chlorine generation and solution-phase oxidation. We observed only a 22.8% Se removal efficiency on the first day of performing the experiment at 80 °C, with an effluent soluble Se level of 5.57 mg L^{-1} (Figure S3C, SI section 5). The Se removal efficiency further drops to 16.9% and 15.3% on the second and third day due to surface-attached conductive Se(0). Hence, our results suggested that four-electron Se(IV) reduction outcompetes the six-electron Se(IV) reduction when treating real FGD wastewater, primarily due to the interference of chlorine-based oxidants.

Electrochemical Se Removal in Simulated Agricultural Drainage. We explored SeDER performance in two different types of simulated agricultural drainage, including raw drainage (87.6 μg L^{-1} Se) and concentrated drainage (175.7 μg L^{-1} Se). As expected, the SeDER performance was notably constrained by worsened mass transport under ultralow Se levels and 3.6 g L^{-1} chloride. For the four-electron Se(IV) reduction, we observed linear kinetics over the 24-h operation (R^2 > 0.99, Figure 5). The effluent Se levels were 67.6 and

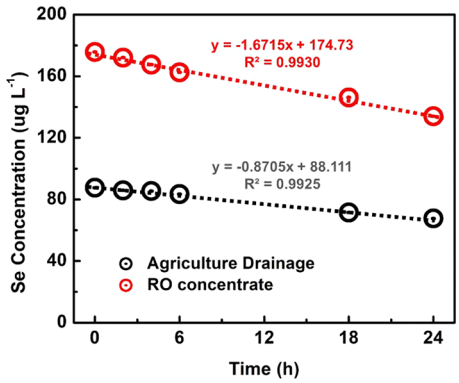

Figure 5. Electrochemical Se(IV) reduction and removal performance through a four-electron Se(IV) reduction in simulated agricultural drainage. The two types of simulated drainage include the raw drainage (87.6 μg L^{-1} Se) and the concentrated drainage (175.7 μg L^{-1} Se).

134.0 μg L^{-1} for raw and concentrated drainage, resulting in a Se removal efficiency of 22.8% and 23.7%, respectively. Similar to trends observed in FGD wastewater, anodic chloride oxidation and solution-phase parasitic reactions severely limited performance in the six-electron Se(IV) reduction pathway at both 20 and 80 °C. The total soluble Se levels decreased from ~75.0 μg L^{-1} to 61.1 μg L^{-1} and 68.7 μg L^{-1} at 20 and 80 °C, respectively, with a Se removal efficiency of 18.5% and 8.4%. The results suggest that electrochemical Se removal using our prototype batch reactor is not competitive for treating ultralow Se wastewaters. Enhancing SeDER removal performance will require that agricultural drainage is concentrated by at least 1 order of magnitude (e.g., through capacitive deionization and electrosorption),[35] while cell design will need to significantly enhance the mass transfer rate of Se oxyanions. Better electrode and cell designs (e.g.,

https://doi.org/10.1021/acsestengg.1c00099
ACS EST Engg. 2021, 1, 1028–1035

functionalized electrode interfaces)[36] could also be coupled with a localized heating strategy to sustain an elevated cathode surface temperature for energy-efficient Se removal.[37]

Perspectives and Implications. In this study, we evaluate both the cathodic and anodic competing ion behavior in a SeDER process. The results suggest that sulfate promotes electrochemical Se(IV) removal in both four- and six-electron pathways, but nitrate slightly hinders Se(IV) removal by occupying reaction sites. The anodic competing ions, especially chloride, decrease SeDER performance by generating strong oxidants and disrupting Se(IV) reduction pathways. We also report that four-electron Se(IV) reduction outperforms six-electron reduction when treating simulated FGD wastewater (with 7 g L^{-1} Cl^-). Ideal operation of our unoptimized electrode and process designs resulted in a minimum effluent Se level of 0.23 mg L^{-1}, a highest removal efficiency of 96.9%, and a threshold deposition capacity of 3.5 g m^{-2}.

To further enhance the energy efficiency of SeDER, we need to significantly enhance the Faradaic efficiency. The Au electrode provides a stable and reusable interface for electrochemical Se reduction, but it also facilitates hydrogen evolution reactions that reduce the Faradaic efficiency. Between the metal M electrode (e.g., Au) and the anchoring group −H (of Au−H, to form H_2) or −O (of Au−O_3Se^-, to form Se(0)), we need to select an electrode material that favors M−O over the M−H. Midrange M−O interaction energy would promote high activity and ensure that the M−O interaction energy is neither too low for Se oxyanion to be easily detached nor too high to be firmly bonded to the metal surface. On the basis of this "volcano-plot" theory, we found that Au has a low interaction energy for both Au−H and Au−O.[26] Instead, we could select iron (Fe) or nickel (Ni) based electrode materials that exhibit a relatively low interaction energy for M−H, but an ideally situated interaction energy for M−O. We are in the process of evaluating these alternative electrode materials to ensure enhanced Faradaic efficiency, consistent Se removal, and lower material costs.

Lacking effective approaches for eliminating chloride from industrial and agricultural wastewater, we need to develop effective strategies for mitigating the effect of anodic chloride oxidation. Compared to the six-electron Se(IV) reduction, the shielding effect of the outer Se(0) layer in four-electrode Se deposition certainly reduces the chlorine-based oxidation when treating the FGD wastewater. However, we did not observe an obvious shielding effect in a four-electron Se(IV) reduction when treating agricultural drainage, likely due to a thinner deposited Se(0) layer. While a two-chamber electrochemical system that decouples the anodic and cathodic reactions could further mitigate the effect of chloride, this design will inevitably increase overall system impedance and capital and maintenance costs. Understanding the trade-offs in capital and operational expenses for the SeDER system relative to those for other Se removal technologies is a critical next step for technology evaluation.

Reactor design, especially cathode design, also requires extensive evaluation in future research. Given that four-electron Se(IV) reduction offers more reliable Se removal in treating warm FGD wastewater, we may realize diminished returns by using a 3-D structured electrode to further enhance the surface area. However, we could significantly enhance mass transfer rate and Se removal/deposition efficiency by converting the current foil electrode to a rotating cylinder electrode. A previous study has reported fast reaction electrochemical kinetics by applying a 600 rpm rotating speed to sustain flow turbulence.[38] A comprehensive analysis should also be performed to evaluate the trade-off between a potentially decreased deposition rate on a rotating electrode and an increase in oxyanion mass transfer, electrochemical reaction rate, and Faradaic efficiency by introducing convection.

■ ASSOCIATED CONTENT

Supporting Information

The Supporting Information is available free of charge at https://pubs.acs.org/doi/10.1021/acsestengg.1c00099.

(1) Details on electrode regeneration and Se deplating; (2) performance of regenerated electrodes; (3) detailed method for quantifying performance metrics; (4) results for cathodic competing ion behavior of sulfate, nitrate, and nitrite in two-component solution matrices; and (5) electrochemical Se(IV) removal in simulated FGD wastewater through a six-electrode reduction pathway (PDF)

Electrode regeneration (MP4)

■ AUTHOR INFORMATION

Corresponding Author

Meagan S. Mauter − *Department of Civil and Environmental Engineering, Stanford University, Stanford, California 94305, United States;* orcid.org/0000-0002-4932-890X; Phone: (650) 725-4911; Email: mauter@stanford.edu

Author

Shiqiang Zou − *Department of Civil and Environmental Engineering, Stanford University, Stanford, California 94305, United States;* orcid.org/0000-0001-9394-8543

Complete contact information is available at: https://pubs.acs.org/10.1021/acsestengg.1c00099

Notes

The authors declare the following competing financial interest(s): The authors disclosed the research results to Stanfords Office of Technology Licensing, and a provisional patent application was submitted. The authors declare no other competing financial interest.

■ ACKNOWLEDGMENTS

This work was partially supported by a faculty startup fund of Stanford University. S.Z. was financially supported by the National Science Foundation (DMR-2023833). We sincerely thank Dr. Alexander V. Dudchenko for his help with the customized 3-D printed lids.

■ REFERENCES

(1) Lemly, A. D. Aquatic selenium pollution is a global environmental safety issue. *Ecotoxicol. Environ. Saf.* **2004**, *59* (1), 44−56.

(2) Kavlak, G.; Graedel, T. E. Global anthropogenic selenium cycles for 1940−2010. *Resour. Conserv. Recycl.* **2013**, *73*, 17−22.

(3) Winkel, L. H. E.; Johnson, C. A.; Lenz, M.; Grundl, T.; Leupin, O. X.; Amini, M.; Charlet, L. Environmental Selenium Research: From Microscopic Processes to Global Understanding. *Environ. Sci. Technol.* **2012**, *46* (2), 571−579.

(4) Petrov, P. K.; Charters, J. W.; Wallschläger, D. Identification and Determination of Selenosulfate and Selenocyanate in Flue Gas Desulfurization Waters. *Environ. Sci. Technol.* **2012**, *46* (3), 1716−1723.

(5) Kushwaha, A.; Goswami, L.; Lee, J.; Sonne, C.; Brown, R. J.; Kim, K.-H. Selenium in soil-microbe-plant systems: Sources, distribution, toxicity, tolerance, and detoxification. *Crit. Rev. Environ. Sci. Technol.* **2021**, 1−42.
(6) Luoma, S. N.; Presser, T. S. Emerging Opportunities in Management of Selenium Contamination. *Environ. Sci. Technol.* **2009**, *43* (22), 8483−8487.
(7) Eisler, R. *Selenium Hazards to Fish, Wildlife, and Invertebrates: a Synoptic Review*; Fish and Wildlife Service, U.S. Department of the Interior, 1985.
(8) Ohlendorf, H. M.; Santolo, G. M.; Byron, E. R.; Eisert, M. A. Kesterson Reservoir: 30 Years of Selenium Risk Assessment and Management. *Integr. Environ. Assess. Manage.* **2020**, *16* (2), 257−268.
(9) Peeters, J. G.; Bonkoski, W. A.; Cote, P. L.; Husain, H.; Pickett, T. M. Apparatus and method for treating FGD blowdown or similar liquids. WO/2007/012181, 2012.
(10) Kratochvil, D.; Mohammadi, F.; Littlejohn, P.; Sanguinetti, D. Removal of dissolved selenium from aqueous solutions. US20160289092A1, 2018.
(11) Golder Associates Ltd. *State-of-Knowledge on Selenium Treatment Technologies*; North American Metals Council - Selenium Working Group: Vancouver, British Columbia, Canada, 2020.
(12) Al Kuisi, M.; Abdel-Fattah, A. Groundwater vulnerability to selenium in semi-arid environments: Amman Zarqa Basin, Jordan. *Environ. Geochem. Health* **2010**, *32* (2), 107−128.
(13) Hyun, S.; Burns, P. E.; Murarka, I.; Lee, L. S. Selenium (IV) and (VI) sorption by soils surrounding fly ash management facilities. *Vadose Zone J.* **2006**, *5* (4), 1110−1118.
(14) Zou, S.; Mauter, M. S. Direct Electrochemical Pathways for Selenium Reduction in Aqueous Solutions. *ACS Sustainable Chem. Eng.* **2021**, *9* (5), 2027−2036.
(15) Gingerich, D. B.; Grol, E.; Mauter, M. S. Fundamental challenges and engineering opportunities in flue gas desulfurization wastewater treatment at coal fired power plants. *Environ. Sci. Water Res. Technol.* **2018**, *4* (7), 909−925.
(16) Gingerich, D. B.; Mauter, M. S. Flue Gas Desulfurization Wastewater Composition and Implications for Regulatory and Treatment Train Design. *Environ. Sci. Technol.* **2020**, *54* (7), 3783−3792.
(17) Bouhadana, Y.; Ben-Tzion, M.; Soffer, A.; Aurbach, D. A control system for operating and investigating reactors: the demonstration of parasitic reactions in the water desalination by capacitive de-ionization. *Desalination* **2011**, *268* (1−3), 253−261.
(18) Liu, W.; Ai, Z.; Zhang, L. Design of a neutral three-dimensional electro-Fenton system with foam nickel as particle electrodes for wastewater treatment. *J. Hazard. Mater.* **2012**, *243*, 257−264.
(19) da Silva, S. W.; Navarro, E. M.; Rodrigues, M. A.; Bernardes, A. M.; Pérez-Herranz, V. The role of the anode material and water matrix in the electrochemical oxidation of norfloxacin. *Chemosphere* **2018**, *210*, 615−623.
(20) Su, W.; Zhang, L.; Tao, Y.; Zhan, G.; Li, D.; Li, D. Sulfate reduction with electrons directly derived from electrodes in bioelectrochemical systems. *Electrochem. Commun.* **2012**, *22*, 37−40.
(21) Jasper, J. T.; Yang, Y.; Hoffmann, M. R. Toxic Byproduct Formation during Electrochemical Treatment of Latrine Wastewater. *Environ. Sci. Technol.* **2017**, *51* (12), 7111−7119.
(22) Li, M.; Feng, C.; Zhang, Z.; Shen, Z.; Sugiura, N. Electrochemical reduction of nitrate using various anodes and a Cu/Zn cathode. *Electrochem. Commun.* **2009**, *11* (10), 1853−1856.
(23) *Final Power Plant Monitoring Data Collected Under Clean Water Act Section 308 Authority*; Eastern Research Group, Inc., 2012.
(24) Bureau of Reclamation, South-Central California Area Office. *San Luis Drainage Feature Reevaluation Demonstration Treatment Facility at Panoche Drainage District (FONSI-10−030)*; U.S. Department of the Interior, 2011.
(25) Duca, M.; Koper, M. T. Powering denitrification: the perspectives of electrocatalytic nitrate reduction. *Energy Environ. Sci.* **2012**, *5* (12), 9726−9742.
(26) Vijh, A. K. Electrocatalysis of the electroreduction of nitric acid by metals. *J. Catal.* **1974**, *32* (2), 230−236.
(27) Ball, S.; Milne, J. Studies on the interaction of selenite and selenium with sulfur donors. Part 3. Sulfite. *Can. J. Chem.* **1995**, *73* (5), 716−724.
(28) Rahim, S.; Milne, J. Studies on the interaction of selenite and selenium with sulphur donors. Part 4. Thiosulfate. *Can. J. Chem.* **1996**, *74* (5), 753−759.
(29) Córdoba, P. Partitioning and speciation of selenium in wet limestone flue gas desulphurisation systems: A review. *Fuel* **2017**, *202*, 184−195.
(30) Castaldi, F. J. Aqueous Behavior of Elements in a Flue Gas Desulfurization Sludge Disposal Site. *Water Encyclopedia* **2005**, *1*, 848−853.
(31) Zuman, P.; Somer, G. Polarographic and voltammetric behavior of selenious acid and its use in analysis. *Talanta* **2000**, *51* (4), 645−665.
(32) Liu, S.; Salhi, E.; Huang, W.; Diao, K.; von Gunten, U. Kinetic and mechanistic aspects of selenite oxidation by chlorine, bromine, monochloramine, ozone, permanganate, and hydrogen peroxide. *Water Res.* **2019**, *164*, 114876.
(33) Lou, Z.; Li, P.; Pan, Q.; Han, K. A reversible fluorescent probe for detecting hypochloric acid in living cells and animals: utilizing a novel strategy for effectively modulating the fluorescence of selenide and selenoxide. *Chem. Commun.* **2013**, *49* (24), 2445−2447.
(34) Peng, D.; Zhang, J.; Liu, Q.; Taylor, E. W. Size effect of elemental selenium nanoparticles (Nano-Se) at supranutritional levels on selenium accumulation and glutathione S-transferase activity. *J. Inorg. Biochem.* **2007**, *101* (10), 1457−1463.
(35) Chen, R.; Sheehan, T.; Ng, J. L.; Brucks, M.; Su, X. Capacitive deionization and electrosorption for heavy metal removal. *Environ. Sci. Water Res. Technol.* **2020**, *6* (2), 258−282.
(36) Candeago, R.; Kim, K.; Vapnik, H.; Cotty, S.; Aubin, M.; Berensmeier, S.; Kushima, A.; Su, X. Semiconducting Polymer Interfaces for Electrochemically Assisted Mercury Remediation. *ACS Appl. Mater. Interfaces* **2020**, *12* (44), 49713−49722.
(37) Dudchenko, A. V.; Chen, C.; Cardenas, A.; Rolf, J.; Jassby, D. Frequency-dependent stability of CNT Joule heaters in ionizable media and desalination processes. *Nat. Nanotechnol.* **2017**, *12* (6), 557.
(38) Belarbi, Z.; Trembly, J. P. Electrochemical processing to capture phosphorus from simulated concentrated animal feeding operations waste. *J. Electrochem. Soc.* **2018**, *165* (13), E685.

https://doi.org/10.1021/acsestengg.1c00099
ACS EST Engg. 2021, 1, 1028−1035